NANO LETTERS

LETTER

pubs.acs.org/NanoLett

Hollow Carbon Nanofiber-Encapsulated Sulfur Cathodes for High Specific Capacity Rechargeable Lithium Batteries

Guangyuan Zheng,[†,||] Yuan Yang,[‡,||] Judy J. Cha,[‡] Seung Sae Hong,[§] and Yi Cui*[,‡,#]

[†]Department of Chemical Engineering, [‡]Department of Materials Science and Engineering, and [§]Department of Applied Physics, Stanford University, Stanford, California 94305, United States

[#]Stanford Institute for Materials and Energy Sciences, SLAC National Accelerator Laboratory, 2575 Sand Hill Road, Menlo Park, California 94025, United States

Supporting Information

ABSTRACT: Sulfur has a high specific capacity of 1673 mAh/g as lithium battery cathodes, but its rapid capacity fading due to polysulfides dissolution presents a significant challenge for practical applications. Here we report a hollow carbon nanofiber-encapsulated sulfur cathode for effective trapping of polysulfides and demonstrate experimentally high specific capacity and excellent electrochemical cycling of the cells. The hollow carbon nanofiber arrays were fabricated using anodic aluminum oxide (AAO) templates, through thermal carbonization of polystyrene. The AAO template also facilitates sulfur infusion into the hollow fibers and prevents sulfur from coating onto the exterior carbon wall. The high aspect ratio of the carbon nanofibers provides an ideal structure for trapping polysulfides, and the thin carbon wall allows rapid transport of lithium ions. The small dimension of these nanofibers provides a large surface area per unit mass for Li_2S deposition during cycling and reduces pulverization of electrode materials due to volumetric expansion. A high specific capacity of about 730 mAh/g was observed at C/5 rate after 150 cycles of charge/discharge. The introduction of $LiNO_3$ additive to the electrolyte was shown to improve the Coulombic efficiency to over 99% at C/5. The results show that the hollow carbon nanofiber-encapsulated sulfur structure could be a promising cathode design for rechargeable Li/S batteries with high specific energy.

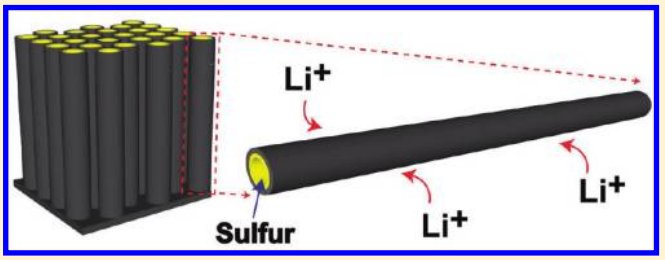

KEYWORDS: Hollow carbon nanofiber-encapsulated sulfur, Li/S batteries, high specific capacity, energy storage

Rechargeable batteries with high specific energy are essential for solving imminent energy and environmental issues. Li-ion batteries have one of the highest specific energies among rechargeable batteries,[1−3] but state-of-the-art technology based on intercalation mechanism has a theoretical specific energy of ∼400 Wh/kg for both $LiCoO_2$/graphite and $LiFePO_4$/graphite systems.[4,5] To achieve higher specific energy, new materials for both the cathode and anode are required. Despite significant progress in the development of high capacity anode materials, such as nanostructured Si,[6−9] the relatively low charge capacity of cathodes remains the limiting factor for commercializing rechargeable batteries with high specific energy. Current cathode materials, such as transition-metal oxides and phosphates, have an inherent limit of 300 mAh/g.[10] On the other hand, sulfur cathodes have a theoretical capacity of 1673 mAh/g. Though its voltage is 2.2 V vs Li/Li^+, which is about 60% of conventional Li-ion batteries, the theoretical specific energy of the Li/S cell is ∼2600 Wh/kg, five times higher than that of the $LiCoO_2$/graphite system.[11] Sulfur also has many other advantages such as low cost and nontoxicity. However, the poor cycle life of Li/S batteries has been a significant hindrance toward its commercialization. The fast capacity fading during cycling is due to a variety of factors, including the dissolution of intermediate lithium polysulfides products (Li_2S_x, $4 \leq x \leq 8$) in the electrolyte,[12] large volumetric expansion of sulfur (∼80%) during cycling, and the insulating nature of Li_2S. In order to improve the cycle life of Li/S batteries, the dissolution of polysulfides is one of the key problems to tackle.[13,14] Polysulfides are soluble in the electrolyte and could diffuse to the lithium anode, resulting in undesired parasitic reactions. The shuttle effect also leads to random precipitation of Li_2S_2 and Li_2S on the positive electrode, which dramatically changes the electrode morphology and thus results in fast capacity fading.[15]

As a result, efficient trapping of polysulfides is highly desired for improving the cycle life of Li/S batteries. Various approaches have been demonstrated, such as surface coating,[16−19] conductive matrix,[20] novel electrolytes,[21,22] and porous carbon.[10,23−26] For example, graphene/polymer coating has been shown to give a smaller capacity decay of 10−15% over 100 cycles with a discharge capacity of 600 mAh/g.[17] Porous carbon is another attractive approach, as it can both trap polysulfides and provide conductive paths for electrons. Nevertheless, a large surface area of sulfur is still exposed to the electrolyte, as the particle size of

Received: August 10, 2011
Revised: September 11, 2011
Published: September 14, 2011

the porous carbon is typically on the order of 1 μm, which causes significant polysulfides dissolution.[14] Based on our own research and literature studies in the past several years, we believe that an ideal structure for sulfur electrode should have the following characteristics: (1) a closed structure for efficient polysulfides containment; (2) limited surface area for sulfur−electrolyte contact; (3) sufficient space to accommodate sulfur volumetric expansion and small characteristic dimension of the sulfur electrode to avoid pulverization; (4) a short transport pathway for both electrons and Li ions to achieve high capacity at a high power rate; (5) a large conductive surface area for depositing insulating Li_2S_2 and Li_2S, in order to preserve the morphology of electrodes;[15] and (6) suitable electrolyte additives to passivate the lithium surface to minimize the shuttle effect. Some of these characteristics require structure designs that are self-conflicting, such as the minimization of sulfur−electrolyte contact and the large surface area needed for Li_2S_2 and Li_2S plating, which explain why it is very challenging to realize sulfur electrodes with high specific capacity and long cycle life.

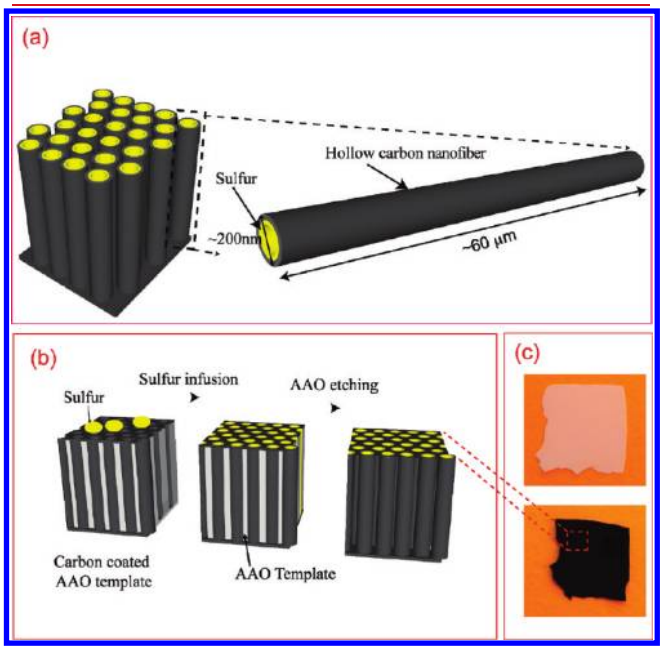

Figure 1. Schematic of design and fabrication process of hollow carbon nanofibers/sulfur composite structure. (a) The design principle showing the high aspect ratio of the hollow carbon nanofiber for effective trapping of polysulfides and (b) the fabrication process of carbon/sulfur cathode structure. (c) Digital camera images showing the contrast of AAO template before and after carbon coating and sulfur infusion.

To address these requirements, we designed a hollow carbon nanofiber-encapsulated sulfur electrode structure, comprising vertical arrays of hollow carbon nanofibers filled with melted sulfur (Figure 1a). Anodic aluminum oxide (AAO) membranes were used as templates for the fabrication of hollow carbon nanofibers, through a polystyrene carbonization process. AAO membranes have been shown to be effective templates for synthesizing nanomaterials in energy applications, due to the large surface area and uniformity of the nanopores.[27−30] In the present structure, the AAO membrane serves as both a template for carbon nanofiber formation and a barrier to prevent sulfur from coating onto the exterior carbon fiber wall. The nanofiber diameters range between 200 and 300 nm, while the length is up to 60 μm, corresponding to the AAO template structure (Figure S1, Supporting Information). Sulfur is effectively contained in the high-aspect-ratio hollow carbon nanofibers, and its contact with the electrolyte is limited to the two openings. The hollow structure also provides large space for sulfur expansion during cycling. As lithium can easily penetrate the thin carbon wall, rapid ionic transport is also possible. The one-dimensional conductive carbon nanofibers enable facile transport of electrons and a large area for depositing Li_2S_2 and Li_2S. These attributes of the hollow carbon nanofiber structure are important in ensuring high specific capacity and stable cycle life of the sulfur cathode in Li/S batteries.

We emphasize that it is important to have sulfur coated only onto the inner surface of hollow carbon nanofibers instead of the exterior surface. Multiwalled carbon nanotubes/sulfur composite

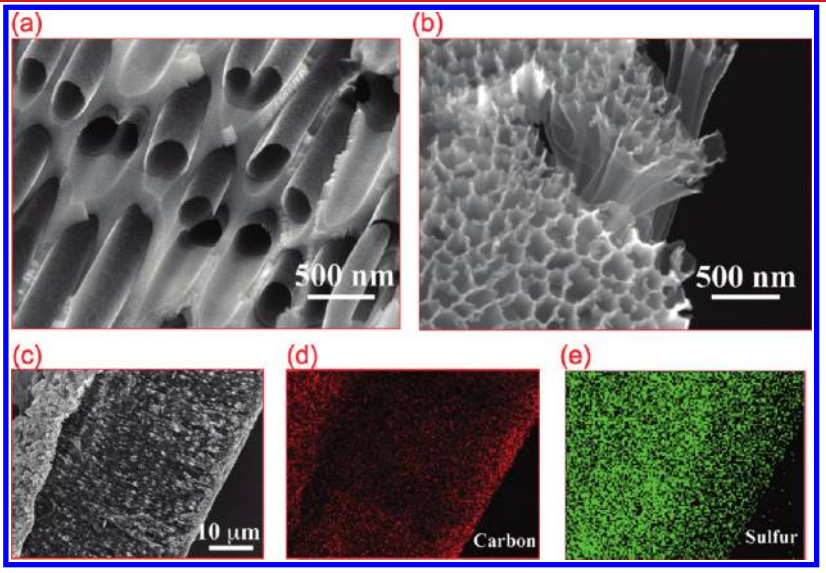

Figure 2. SEM characterizations of hollow carbon nanofiber-encapsulated sulfur. (a) AAO template after carbon coating. (b) Hollow carbon nanofiber-encapsulated sulfur after etching away AAO template. (c) Cross-sectional image of hollow carbon nanofiber/S array and elemental mapping of carbon (d) and sulfur (e) of (c).

dx.doi.org/10.1021/nl2027684 |*Nano Lett.* 2011, 11, 4462–4467

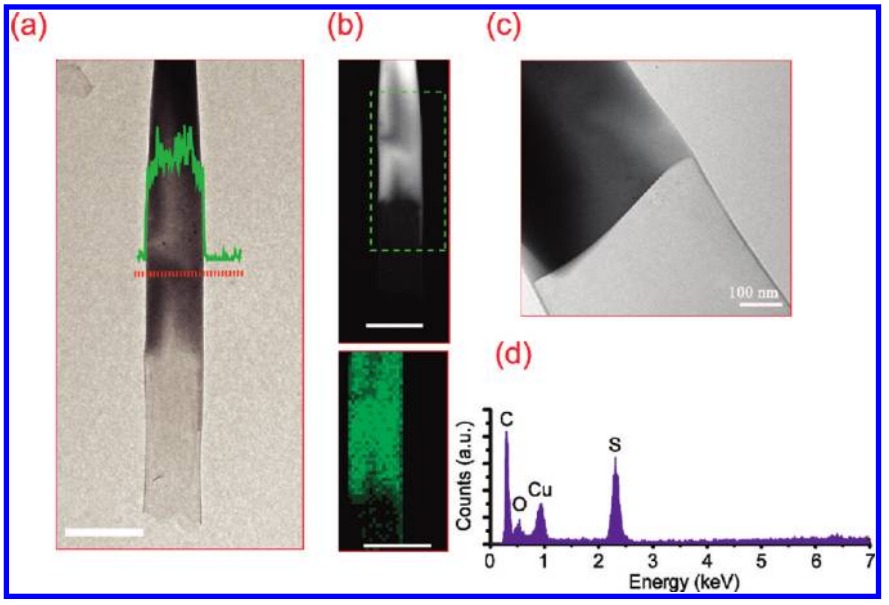

Figure 3. TEM characterizations of hollow carbon nanofiber-encapsulated sulfur. (a) Bright field TEM image of an individual nanofiber. The green line represents counts of sulfur signal along the dashed orange line. (b) Dark field STEM image (up) and EDS mapping of sulfur (down, in green) of the nanofiber. (c) Zoom-in image of another sulfur-filled carbon nanofiber, showing the thin carbon wall. (d) The corresponding average EDS spectrum obtained from the nanofiber in (c). Scale bars in (a) and (b) are both 500 nm.

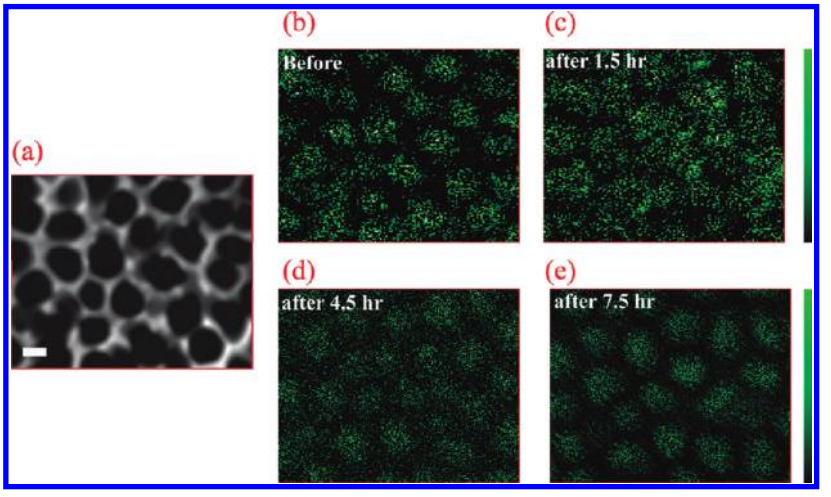

Figure 4. AES of the AAO/carbon template filled with sulfur, before and after sputtering with Ar ions. (a) SEM image of the top view of carbon coated AAO template after infusion of sulfur. The scale bar is 200 nm. Elemental mapping of sulfur (b) before Ar sputtering and (c) 1.5 h, (d) 4.5 h, and (e) 7.5 h after sputtering. The sputtering rate is about 3.3 μm/h.

have previously been demonstrated but sulfur was mainly coated onto the outer surface.[31−33] Consequently sulfur was exposed to the electrolyte without any capping, and the dissolution issue was not solved. To tackle this issue, we used a template-assisted method to fabricate a cathode structure with sulfur only coated on the inner wall of the carbon fibers, as shown in Figure 1b. AAO template (Whatman, pore size ~200 nm, thickness ~60 μm) was used as the template for making hollow carbon nanofibers. Typically, 120 mg of AAO membrane was placed inside an alumina boat, and 2 mL of 10 wt % of polystyrene (PS) suspended in dimethylformamide (DMF) was dropped onto the template as the carbon precursor. The carbonization was done by heating the AAO/PS/DMF mixture at 750 °C for 4 h under a slow flow of N_2 gas. After cooling down, carbon-coated AAO template was loaded into a small glass vial, together with a controlled amount of 1% sulfur solution in toluene. The sample was dried in a vacuum oven, before being heated up to 155 °C and kept for 12 h to ensure uniform sulfur diffusion into the carbon fibers. To remove the AAO template, the AAO/carbon nanofiber/sulfur composite is immersed in 2 M of H_3PO_4 solution for 10 h. Figure 1c shows the digital camera images of pristine AAO template before (white) and after (black) carbon coating and sulfur infusion, indicating that sulfur was absorbed into the hollow carbon fibers.

Scanning electron microscopy (SEM) images of the designed structures at different stages of fabrication are shown in Figure 2. After carbon coating at 750 °C, continuous hollow carbon nanofibers were formed inside the AAO template (Figure 2a).

dx.doi.org/10.1021/nl2027684 |*Nano Lett.* 2011, 11, 4462–4467

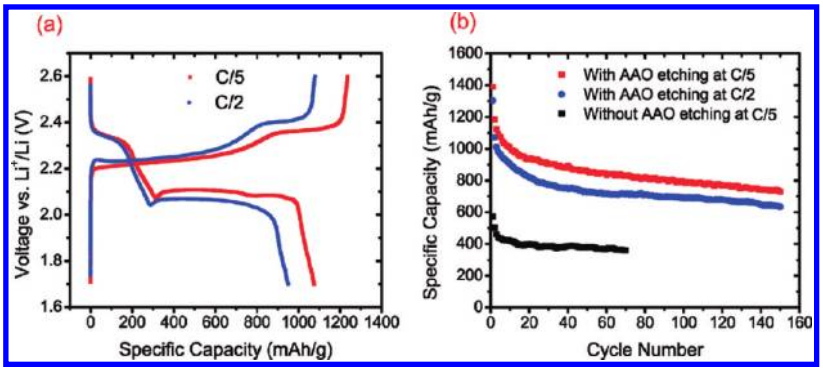

Figure 5. Electrochemical performance of the carbon nanofiber-encapsulated sulfur cathodes. (a) Typical charge/discharge voltage profiles at C/5 and C/2. (b) Cycle life at C/5 and C/2, as compared to a control sample in which the AAO was not etched away. The voltage range is 1.7−2.6 V vs Li/Li^+.

The weight gain after carbon coating was about 2% of the AAO template. Figure 2b shows the image of hollow carbon nanofibers after sulfur infusion and AAO etching. Typically, the weight ratio of sulfur to carbon was 3:1 in the final electrode structure, corresponding to a 75 v% of sulfur content in the composite. The sulfur loading was controlled so that there was enough free space for sulfur to expand during the formation of Li_2S. To confirm the presence of carbon and sulfur, energy-dispersive X-ray spectroscopy (EDS) mappings were performed over the cross-section of the whole carbon nanofiber array, with the corresponding SEM image in Figure 2c. Carbon (Figure 2d) and sulfur (Figure 2e) signals were detected uniformly over the whole cross-section, validating our structural design and indicating that sulfur was well distributed within the hollow carbon nanofibers.

Further evidence of sulfur containment within the carbon nanofiber was provided by the transmission electron microscopy (TEM) images. Figure 3a shows a hollow carbon nanofiber with sulfur encapsulated inside. Sulfur appears darker under TEM, as it is heavier than carbon. An EDS line scan (dashed orange line) across the carbon nanofiber further confirmed the presence of sulfur. The green spectrum represents the counts of sulfur signal along the dashed line. The spectrum shows clearly that sulfur is present only inside the hollow carbon nanofibers but not outside. This is also verified by the sulfur EDS mapping in Figure 3b. The full EDS spectrum over the whole tube (Figure 3d) shows clearly the carbon and sulfur peaks but not any aluminum signal, indicating that there is no or very little alumina residue left from the AAO template. The zoom-in image (Figure 3c) of another carbon nanofiber shows the fiber wall has a thickness of only 8−9 nm, which is important in allowing fast kinetics of lithium ion diffusion.

Spatial distribution of sulfur inside the hollow carbon nanofiber arrays is further demonstrated by auger electron spectroscopy (AES) with Ar ion sputtering. Figure 4a shows the top view SEM image of the nanofiber array, revealing the hexagonal packing. The elemental mapping of sulfur before sputtering (Figure 4b) also gave similar hexagonal pattern, suggesting that sulfur was present in the hollow channels. Figure 4c−e shows the sulfur elemental mappings after 1.5, 4.5, and 7.5 h of Ar ion sputtering, respectively. Around 25 μm, of the sample was etched away after 7.5 h of sputtering. The variation in the sulfur mapping patterns was due to the change in the AAO channel morphology at different depths (Figure S1, Supporting Information). The hexagonal packing became much clearer at regions closer to the center of the hollow nanofiber array. The AES mappings show that globally sulfur is well distributed from the top to deep inside the hollow carbon nanofibers.

The above characterizations clearly show that hollow carbon nanofiber-encapsulated sulfur was formed with the assistance of the AAO template. To further understand the crystal structure of carbon and sulfur in the final structure, Raman spectroscopy and X-ray diffraction (XRD) were perform to study the as-fabricated sulfur electrode. The Raman measurement shows a typical spectrum of partially graphitized carbon, indicated by the G band (1600 cm^{-1}) and D band (1360 cm^{-1})[34] in Figure S2, Supporting Information. The G band features the in-plane vibration of sp^2 carbon atoms, and the D band originates from the defects. The coexistence of the two bands indicated that the carbon was partially graphitized with some defects and disorders. The absence of sulfur peak in the Raman spectrum of the final electrode structure indicates that sulfur was well encapsulated in the hollow nanofibers.

XRD pattern (Figure S3, Supporting Information) of the carbon/sulfur composites only shows a weak peak at 23.05°, corresponding to the strongest (222) peak of orthorhombic sulfur (PDF 00-001-0478). This indicates that sulfur in the hollow nanofibers was very poorly crystallized, which was consistent with previous observations that confined sulfur was less crystalline.[10,35] We notice that there is no peak related to crystalline Al_2O_3 phase in the XRD pattern, indicating that the AAO template was still amorphous after carbonization at 750 °C. This is crucial for the etching of Al_2O_3. In contrast, AAO template heated to 780 °C was difficult to remove, and extra peaks appear in the XRD pattern, suggesting that AAO has transformed into a crystalline phase (Figure S4, Supporting Information).

To evaluate the electrochemical performance of hollow carbon nanofiber-encapsulated sulfur, 2032-type coin cells (MTI) were fabricated. The prepared sample was pressed onto an aluminum substrate as the working electrode without any binder or conductive additives. Lithium was used as the counter electrode. The electrolyte was 1 M of lithium bis(trifluoromethanesulfonyl)imide (LiTFSI) in 1,3-dioxolane and 1,2-dimethoxyethane (volume ratio 1:1). The typical mass loading was 1.0 mg sulfur/cm^2, and the specific capacities were calculated based on the sulfur mass only.

The voltage profiles of hollow carbon nanofiber/sulfur composites at different current rates are shown in Figure 5a. The discharge/charge profiles of both C/5 and C/2 (1C=1673 mA/g) show the typical two-plateau behavior of a sulfur cathode, corresponding to the formation of long-chain polysulfides (Li_2S_x, $4 \leq x \leq 8$) at 2.3 V and short-chain Li_2S_2 and Li_2S at 2.1 V. Moreover, the second plateau is flat, suggesting a uniform

dx.doi.org/10.1021/nl2027684 |*Nano Lett.* 2011, 11, 4462–4467

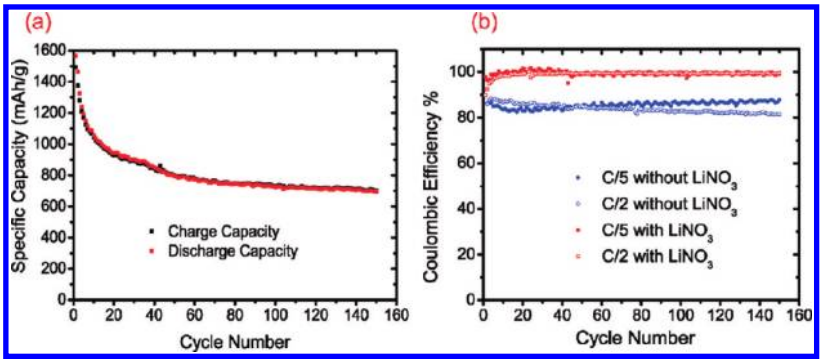

Figure 6. Electrochemical performance of the carbon nanofiber-encapsulated sulfur electrode in electrolyte with $LiNO_3$ additive. (a) Capacities for charge/discharge cycling at C/5. (b) Comparison of Coulombic efficiencies for samples with and without $LiNO_3$ additive in the electrolyte, for cycling at C/5 and C/2.

deposition of Li_2S with little kinetic barriers. It was also observed that the cycling capacity drop was small (~5%) when the current rate increases from C/10 to C/5 after four cycles (Figure S5, Supporting Information), indicating good kinetics of the working electrode. This could be attributed to the high quality of carbon and the thin carbon fiber wall, which significantly improved electronic and ionic transport at the cathode.

Cycling performance at C/5 and C/2 is presented in Figure 5b, together with that of the same carbon hollow fiber/sulfur composite without removing AAO template. With AAO etched away, the cathode structure showed impressive capacity retention. At C/5, the reversible capacity was more than 900 mAh/g after 30 cycles of charge/discharge. This is higher than the results reported for silica colloidal monolith (SCM) derived carbon/sulfur composite, which shows a discharge capacity of around 500 mAh/g after 30 cycles at C/5.[14] A reversible capacity of around 730 mAh/g was observed after 150 cycles of charge/discharge. The discharge capacity at C/2 also shows good cycling stability, and the reversible capacity was around 630 mAh/g after 150 cycles. These results show improved performance in specific capacity as compared to our previous study on graphene-wrapped sulfur cathode structures.[17] In the control sample where the AAO template was not etched away, the electrode has a much lower stable capacity of about 380 mAh/g. Interestingly, the cycling stability of the nonetched sample was slightly better, as the capacity stabilized after 15 cycles of charge/discharge, and the decay was only about 3% for the next 30 cycles before leveling off. This shows that the removal of AAO template is necessary to improve charge transfer through the sidewall of the carbon fibers to achieve high cycling capacity, but at the same time, alumina can potentially help trap polysulfides to improve the cycle life.[36] The mechanical support provided by the AAO template could have also enhanced the stability of the cathode structure. Further optimization of the etching time could realize the possibility of a sulfur electrode with better specific capacity and cycle life.

To further improve the battery performance, 0.1 mol/L of $LiNO_3$ was added to the electrolyte as additive. $LiNO_3$ has been shown to passivate the surface of lithium anode and thus reduce the shuttle effect.[15,37] Figure 6a shows that in the presence of $LiNO_3$, the initial discharge capacity was around 1560 mAh/g, approaching the theoretical capacity of sulfur. The cycling stability is similar to the samples without $LiNO_3$ additive. More importantly, the average Coulombic efficiency increases significantly from 84% to over 99% at C/5 and from 86% to 98% at C/2 (Figure 6b). The improvement in Coulombic efficiency confirms that the $LiNO_3$ additive can significantly reduce polysulfides reaction at the lithium anode and thus the shuttle effect. The combination of rational design of cathode structure and electrolyte additives can achieve a high specific capacity sulfur cathode with stable cycling performance and high Coulombic efficiency.

In summary, we have developed hollow carbon nanofiber-encapsulated sulfur cathodes to achieve high-performance Li/S batteries. In this rational design, sulfur was only coated onto the inner wall of carbon nanofibers by utilizing an AAO template. The high aspect ratio of hollow carbon nanofibers reduces the random diffusion of polysulfides in the organic electrolyte, while the thin carbon wall allows fast transport of lithium ions. A reversible capacity of around 730 mAh/g was observed after 150 cycles of charge/discharge at C/5. Addition of $LiNO_3$ to the electrolyte significantly improved the Coulombic efficiency to 98% and 99% at C/2 and C/5, respectively. Our results show that the hollow carbon nanofiber-encapsulated sulfur cathode structure could be a very promising candidate for high-performance Li/S batteries.

■ ASSOCIATED CONTENT

Ⓢ Supporting Information. Fabrication details of the hollow carbon nanofiber-encapsulated sulfur cathodes, Raman and XRD characterization and supplementary electrochemical data are included. This material is available free of charge via the Internet at http://pubs.acs.org.

■ AUTHOR INFORMATION

Corresponding Author
*E-mail: yicui@stanford.edu.

Author Contributions
‖These authors contributed equally.

■ ACKNOWLEDGMENT

A portion of this work was supported by the Department of Energy, Office of Basic Energy Sciences, Division of Materials Sciences and Engineering under contract DE-AC02-76SF0051 through the SLAC National Accelerator Laboratory LDRD project. Y.C. acknowledges support from King Abdullah University of Science and Technology (KAUST) Investigator Award (no. KUS-l1-001-12). We thank Yu Lin at Stanford University for help with Raman spectroscopy. G.Z. acknowledges financial support from Agency for Science, Technology and Research

(A*STAR), Singapore. Y.Y. acknowledges financial support from a Stanford Graduate Fellowship (SGF).

REFERENCES

(1) Tarascon, J. M.; Armand, M. *Nature* **2001**, *414*, 359–367.
(2) Arico, A. S.; Bruce, P.; Scrosati, B.; Tarascon, J. M.; Van Schalkwijk, W. *Nat. Mater.* **2005**, *4*, 366–377.
(3) Whittingham, M. S. *Chem. Rev. (Washington, DC, U. S.)* **2004**, *104*, 4271–4301.
(4) Kang, B.; Ceder, G. *Nature* **2009**, *458*, 190–193.
(5) Chung, S. Y.; Bloking, J. T.; Chiang, Y. M. *Nat. Mater.* **2002**, *1*, 123–128.
(6) Chan, C. K.; Peng, H.; Liu, G.; McIlwrath, K.; Zhang, X. F.; Huggins, R. A.; Cui, Y. *Nat. Nano* **2008**, *3*, 31–35.
(7) Cui, L. F.; Yang, Y.; Hsu, C. M.; Cui, Y. *Nano Lett.* **2009**, *9*, 3370–3374.
(8) Magasinski, A.; Dixon, P.; Hertzberg, B.; Kvit, A.; Ayala, J.; Yushin, G. *Nat. Mater.* **2010**, *9*, 353–358.
(9) Hu, Y. S.; Demir-Cakan, R.; Titirici, M. M.; Muller, J. O.; Schlogl, R.; Antonietti, M.; Maier, J. *Angew. Chem., Int. Ed.* **2008**, *47*, 1645–1649.
(10) Ji, X. L.; Lee, K. T.; Nazar, L. F. *Nat. Mater.* **2009**, *8*, 500–506.
(11) Joongpyo, S.; Striebel, K. A.; Cairns, E. J. *J. Electrochem. Soc.* **2002**, *149*, A1321–1325.
(12) Mikhaylik, Y. V.; Akridge, J. R. *J. Electrochem. Soc.* **2004**, *151*, A1969–A1976.
(13) Ji, X. L.; Nazar, L. F. *J. Mater. Chem.* **2010**, *20*, 9821–9826.
(14) Ji, X.; Evers, S.; Black, R.; Nazar, L. F. *Nat. Commun.* **2011**, *2*, 325.
(15) Barchasz, C.; Lepretre, J. C.; Alloin, F.; Patoux, S. *J. Power Sources* **2011**, doi: 10.1016/j.jpowsour.2011.07.021.
(16) Choi, Y. J.; Chung, Y. D.; Baek, C. Y.; Kim, K. W.; Ahn, H. J.; Ahn, J. H. *J. Power Sources* **2008**, *184*, 548–552.
(17) Wang, H.; Yang, Y.; Liang, Y.; Robinson, J. T.; Li, Y.; Jackson, A.; Cui, Y.; Dai, H. *Nano Lett.* **2011**, *11*, 2644–2647.
(18) Wu, F.; Chen, J. Z.; Chen, R. J.; Wu, S. X.; Li, L.; Chen, S.; Zhao, T. *J. Phys. Chem. C* **2011**, *115*, 6057–6063.
(19) Cao, Y. L.; Li, X. L.; Aksay, I. A.; Lemmon, J.; Nie, Z. M.; Yang, Z. G.; Liu, J. *Phys. Chem. Chem. Phys.* **2011**, *13*, 7660–7665.
(20) Wang, J. L.; Yang, J.; Xie, J. Y.; Xu, N. X. *Adv. Mater. (Weinheim, Ger.)* **2002**, *14*, 963.
(21) Yuan, L. X.; Feng, J. K.; Ai, X. P.; Cao, Y. L.; Chen, S. L.; Yang, H. X. *Electrochem. Commun.* **2006**, *8*, 610–614.
(22) Shin, J. H.; Cairns, E. J. *J. Power Sources* **2008**, *177*, 537–545.
(23) Liang, C. D.; Dudney, N. J.; Howe, J. Y. *Chem. Mater.* **2009**, *21*, 4724–4730.
(24) Jayaprakash, N.; Shen, J.; Moganty, S. S.; Corona, A.; Archer, L. A. *Angew. Chem., Int. Ed.* **2011**, *123*, 6026–6030.
(25) Yang, Y.; McDowell, M. T.; Jackson, A.; Cha, J. J.; Hong, S. S.; Cui, Y. *Nano Lett.* **2010**, *10*, 1486–1491.
(26) Zhang, B.; Qin, X.; Li, G. R.; Gao, X. P. *Energy Environ. Sci.* **2010**, *3*, 1531–1537.
(27) Che, G.; Lakshmi, B. B.; Martin, C. R.; Fisher, E. R.; Ruoff, R. S. *Chem. Mater.* **1998**, *10*, 260–267.
(28) Che, G.; Lakshmi, B. B.; Fisher, E. R.; Martin, C. R. *Nature* **1998**, *393*, 346–349.
(29) Che, G.; Jirage, K. B.; Fisher, E. R.; Martin, C. R.; Yoneyama, H. *J. Electrochem. Soc.* **1997**, *144*, 4296–4302.
(30) Park, M.-H.; Kim, M. G.; Joo, J.; Kim, K.; Kim, J.; Ahn, S.; Cui, Y.; Cho, J. *Nano Lett.* **2009**, *9*, 3844–3847.
(31) Yuan, L. X.; Yuan, H. P.; Qiu, X. P.; Chen, L. Q.; Zhu, W. T. *J. Power Sources* **2009**, *189*, 1141–1146.
(32) Han, S. C.; Song, M. S.; Lee, H.; Kim, H. S.; Ahn, H. J.; Lee, J. Y. *J. Electrochem. Soc.* **2003**, *150*, A889–A893.
(33) Zheng, W.; Liu, Y. W.; Hu, X. G.; Zhang, C. F. *Electrochim. Acta* **2006**, *51*, 1330–1335.
(34) Ferrari, A. C.; Meyer, J. C.; Scardaci, V.; Casiraghi, C.; Lazzeri, M.; Mauri, F.; Piscanec, S.; Jiang, D.; Novoselov, K. S.; Roth, S.; Geim, A. K. *Phys. Rev. Lett.* **2006**, *97*, 1874011–1874014.
(35) Zhang, B.; Chen, S.; Gao, X. *J. Electrochem.* **2010**, *16*, 35–38.
(36) Choi, Y. J.; Jung, B. S.; Lee, D. J.; Jeong, J. H.; Kim, K. W.; Ahn, H. J.; Cho, K. K.; Gu, H. B. *Phys. Scr.* **2007**, *T129*, 62–65.
(37) Aurbach, D.; Pollak, E.; Elazari, R.; Salitra, G.; Kelley, C. S.; Affinito, J. *J. Electrochem. Soc.* **2009**, *156*, A694–A702.